JOURNAL OF PROPULSION AND POWER
Vol. 12, No. 1, January–February 1996

Mixing of Swirling Jets in a Supersonic Duct Flow

D. K. Kraus* and A. D. Cutler†
George Washington University and NASA Langley Research Center, Hampton, Virginia 23681

Hydrogen fuel injected into a scramjet combustor must mix rapidly if complete combustion is to occur within a reasonable streamwise distance. An experiment has been conducted to determine whether the addition of swirl will improve the mixing of a supersonic jet of fuel simulant (helium or air) injected at 30 deg to the wall into a confined Mach 2 airflow. The swirling jets were created by injecting the fuel simulant tangentially into a cylindrical chamber and accelerating it through a convergent–divergent nozzle. The flow was visualized by imaging Rayleigh scattering from a laser light sheet, and the plume penetration and cross-sectional area were obtained. The plumes from the swirling and nonswirling jets had comparable penetration and area, but the swirling jets contained substantially less mass flow, suggesting better mixing efficiency. Interaction of streamwise vorticity within the plumes of the swirling jets with their images in the duct wall caused the plumes to be inclined laterally to the freestream.

Nomenclature

A = cross-sectional area
d = fuel jet diameter at nozzle exit
M = Mach number
$\dot{m}$ = fuel simulant mass flow rate
p = pressure
p_{eb} = effective backpressure
q_j = fuel simulant mean dynamic pressure, $\frac{1}{2}\dot{m}_j u_j / A_j$
q_∞ = duct dynamic pressure ahead of injector, $\frac{1}{2}\rho_\infty u_\infty^2$
u = x-component velocity
v_θ = edge tangential velocity at the fuel injector nozzle exit
x = streamwise coordinate, Fig. 1
y = transverse coordinate measured from injector axis
z = duct surface normal coordinate, Fig. 1
γ = ratio of specific heat capacities
ρ = density

Subscripts
eff = quantity based on effective fuel jet diameter
j = jet quantity at the jet–nozzle exit
p = fuel simulant plume quantity
0 = stagnation quantity
∞ = duct freestream quantity ahead of injector

Introduction

TO maximize scramjet thrust, fuel must be well mixed in the combustor so that combustion is nearly complete, and stagnation pressure losses must be minimized. Fuel mixing is rapid, but stagnation pressure losses are large if fuel is injected perpendicular to the airstream. If fuel is injected parallel to the airstream, then the direct thrust of the fuel jet is recovered as engine thrust and stagnation pressure losses are minimized, but the mixing is slow.[1] It is expected that fuel mixing in a parallel or nearly parallel injection configuration can be enhanced by addition of swirl to the fuel jet. Compressible mixing-layer growth rates are increased by swirl[2–6] and, if swirling jets are intersected by shock waves (e.g., when the jet nozzle exit pressure is not matched), vortex breakdown can occur generating additional turbulence and mixing.[2–4,7,8] Note that shock (compression) waves produce losses and should be minimized where possible, but they are probably inevitable in any practical supersonic combustor.

The objective of this study was to investigate, in a nonreacting flow, the enhancement of mixing that occurs when swirl is added to a fuel jet in a scramjet-like configuration. A fuel simulant, helium or air, was injected as a jet at 30 deg to the surface into a confined Mach 2 airflow with the static pressure of the jet, in most cases, being matched to the effective backpressure of the main flow. This configuration was chosen both for its geometrical simplicity and because 30-deg wall jets are already known to provide both good mixing and a major thrust component parallel to the airstream,[9–12] the study therefore represents an effort to improve upon a fuel injection concept that may already have practical application. The flows were visualized by imaging Rayleigh scattering from a laser light sheet. For dry gases the intensity of Rayleigh scattering was proportional to air density (helium was essentially invisible). In some cases the fuel simulant was seeded with small quantities of water so that scattering from submicron condensate particles dominated molecular scattering, allowing the fuel plume to be visualized. Penetration and plume cross-sectional area were inferred from these images.

Experimental Method

The facility consisted of a high-pressure plenum, a Mach 2.0 convergent–divergent nozzle, and a constant-area duct of adjustable length with a 1.52 by 3.46 in. cross section (shown in Fig. 1), which simulated the combustor. The boundary-layer displacement thickness at the start of the duct was calculated to be about 0.007 in. and the unit Reynolds number was 2.9×10^7/ft. The jet was created by injecting fuel simulant tangentially through a top-hat-shaped insert (see Fig. 2) into a cylindrical "swirl" chamber and accelerating it through an axisymmetric convergent–divergent nozzle of 0.177-in. throat diameter and 0.25-in. exit diameter. The jet nozzle contour was parallel at its exit, but was not designed, e.g., by the method of characteristics, to produce exactly parallel flow at its exit. The duct static pressure ahead of the injection point was set to atmospheric and the static pressure, measured by a wall static tap within the jet nozzle at the nozzle exit, was set to the effective backpressure (matched pressure) or, in some cases, to twice the effective backpressure (twice the matched pressure). The effective backpressure is usually defined as the pressure behind the shock created by the injected jet, but in practice it depends upon position and upon injec-

Received July 15, 1994; revision received May 26, 1995; accepted for publication June 1, 1995.

*Graduate Research Scholar Assistant, Joint Institute for the Advancement of Flight Sciences; currently at Stanford Telecommunications, Reston, VA. Member AIAA.

†Assistant Professor, Joint Institute for the Advancement of Flight Sciences. Senior Member AIAA.

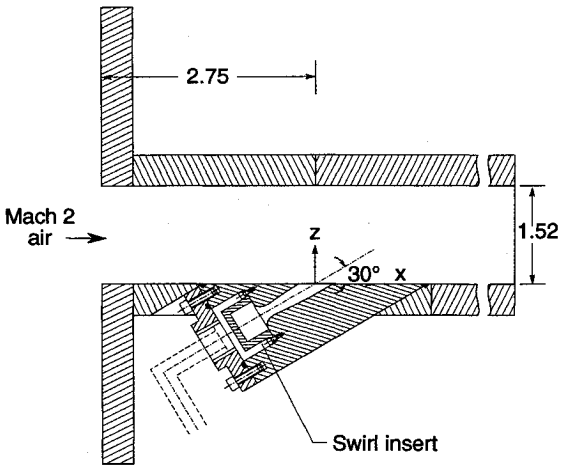

Fig. 1 Section through the fuel injector and duct.

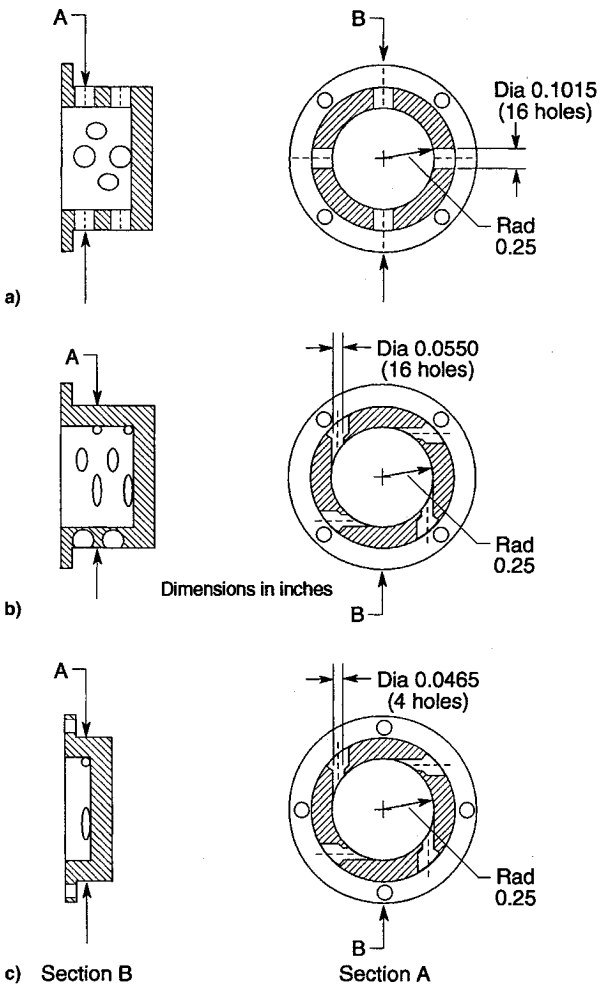

Fig. 2 Swirl inserts: a) straight, b) low swirl, and c) high swirl.

tion pressure, and is not uniquely defined for a given injector geometry. Therefore, following previous practice for 30-deg injection,[10] the effective backpressure was taken to be 80% of the pressure on a 30-deg cone in a flow with the same Mach number and pressure as in the duct: thus, p_{eb} = 33.0 psia given p_∞ = 14.7 psia. Both air and helium were used as fuel simulants to provide a range of fuel simulant to airstream density ratios. Dry compressed air (3–10-ppm water) at ambient temperature (40–65°F) was supplied from a central compressor station and helium was supplied at ambient temperature from high-pressure bottles.

Three interchangeable top-hat inserts, shown in Fig. 2, provided three different swirl rates: the straight insert had radial holes and produced no swirl; the low-swirl and high-swirl inserts had tangential holes. The experimental cases, summarized in Table 1, included three matched pressure cases with helium fuel simulant and two with air; additionally, there was one air case with twice the matched pressure. The quantities v_θ and u_j for helium and air fuel simulants, and $\dot{m}_j$ for helium fuel simulant, were calculated based on the insert and nozzle geometries given jet plenum stagnation conditions and assuming inviscid, irrotational flow with zero radial velocity in the fuel jet nozzle. It follows from these assumptions that the axial component velocity was constant in the radial direction (even with swirl).[2,3] Previous comparisons of such calculations with experiments[3,13] are reasonable within the inviscid part of the jet. Apparently the viscous core (which is contained within a region of low density, and therefore, has a relatively small mass flow), does not upset the mass balance. Calculations of v_θ have an uncertainty of about 20%, u_j of about 10%, and $\dot{m}_j$ of about 8%. For air fuel simulant, $\dot{m}_j$ was directly measured in a separate calibration with an uncertainty of less than 1%. Note that the axial velocity was fairly independent of swirl, but the mass flow rate was substantially reduced by swirl as a result of low density near the axis of the jet. The duct conditions ahead of injection were calculated based on a Mach number of 2.0 and the measured plenum stagnation conditions.

The following independent nondimensional parameters are likely to be important in simulating the penetration and mixing of hydrogen fuel injected into an actual scramjet combustor: M_∞, p_j/p_∞, q_j/q_∞, u_j/u_∞, γ_j, γ_∞, and injector internal and duct geometry.[14] (Note that in Table 1, the jet dynamic pressure is defined by $q_j = \frac{1}{2}\dot{m}_j u_j/A$. The difference between this definition and the conventional one is significant in the swirling cases where density varies radially in the jet.) The duct Mach number of 2.0 is probably typical of a scramjet at flight Mach number of about 6–7; γ_∞ is close to full-scale conditions in the experiment, but, with helium as the fuel simulant, γ_j is not matched. (It is likely that the effects of independently varying γ_j are less than the effects of varying the other parameters.) The remaining parameters are matched when the fuel is simulated by helium if the ratio of fuel stagnation temperature to air stagnation temperature in the scramjet is about 0.4, which may be realistic under certain conditions, or when the fuel is simulated by air if this ratio is about 0.07, which is probably not realistic. Comparison of results from the different fuel simulants provides insight as to the effect of the parameter u_j/u_∞ (the shear), which differs dramatically between air and helium. We have not attempted to model either the inlet boundary layer (the inlet profiles of velocity and pressure, if nonuniform) or the effects of combustion heat release and coupled pressure gradients, which will also influence mixing in a scramjet combustor.

The flow in the duct was visualized by imaging Rayleigh scattering from a laser light sheet, looking at 90 deg to the sheet. The laser was a 10-ns pulsed Nd:YAG with frequency quadrupled output of about 25 mJ per pulse. The wavelength of 266 nm, rather than the more convenient 532 nm, was utilized in order to minimize interference by dust particles.[2] A plano-convex cylindrical lens and a plano-convex spherical lens mounted on a moveable rail formed a light sheet (thickness ~100 μm) at any desired position within the flow. When the light sheet was located at the fuel injector, as described next, a quarter-wave plate was used to provide the proper polarization. The Rayleigh scattering cross section of helium is about 1.5% that of air, thus, in mixtures of helium and air, the Rayleigh scattering intensity is essentially proportional to air number density alone. In some cases the fuel simulant was seeded with roughly 100 ppm of water vapor by spraying liquid water into the fuel simulant supply pipe, where it evaporated. The water vapor condensed in the jet nozzle to form small

Table 1 Measured and calculated parameters

	Straight			Low swirl		High swirl
	Air	Air, 2×[a]	Helium	Air	Helium	Helium
$(p/p_0)_j$	0.116	0.116	0.0985	0.0771	0.0707	0.0240
v_θ/u_j	0	0	0	0.258	0.279	0.513
u_j/u_∞	1.05	1.05	2.77	1.07	2.74	2.68
$\dot{m}_j/(\rho_\infty u_\infty A)$	2.58	5.15	1.36	1.83	0.938	0.647
q_j/q_∞	2.71	5.41	3.77	1.96	2.57	1.73

[a]Jet exit pressure is 2 times effective backpressure.

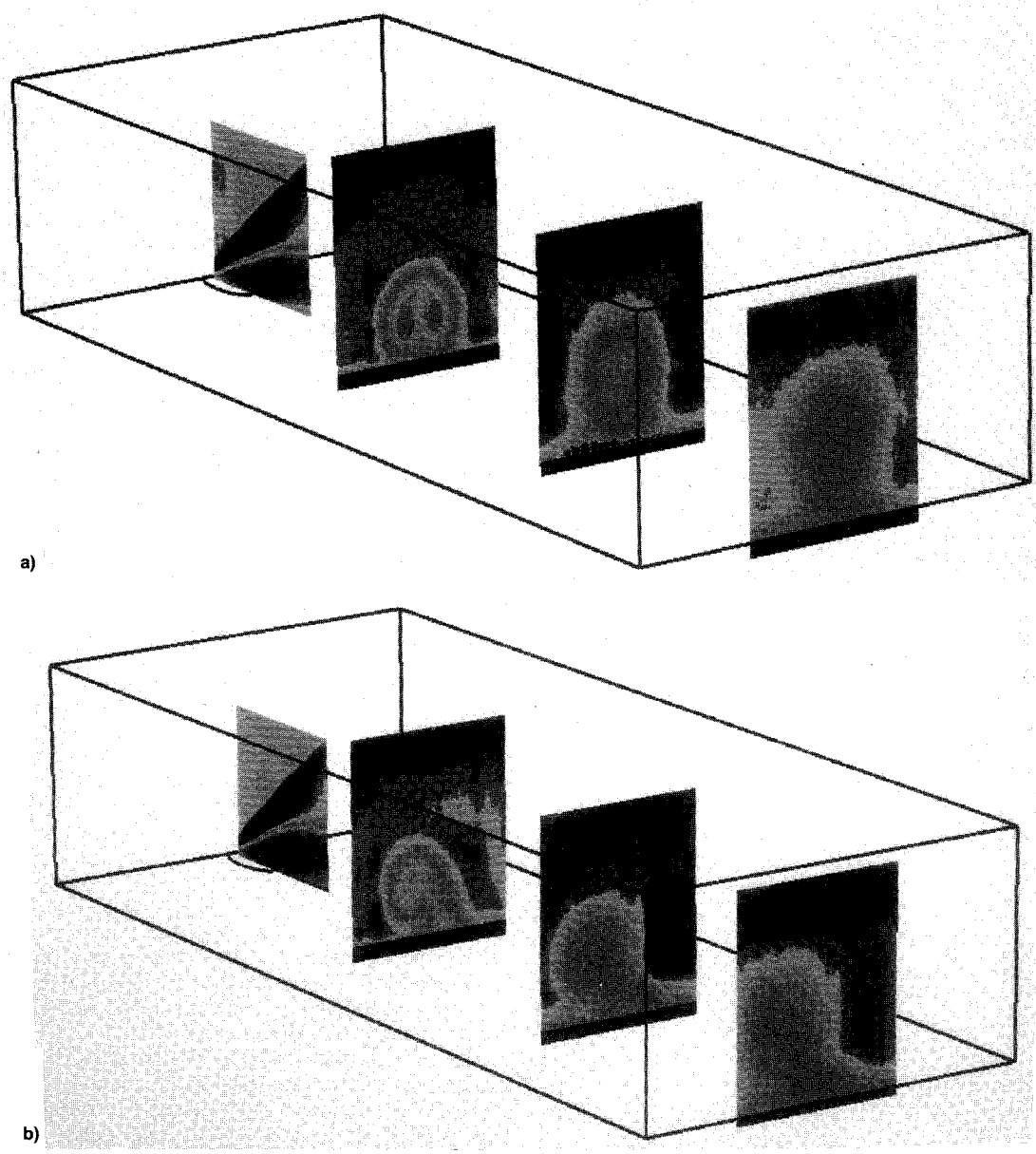

Fig. 3 Three-dimensional view showing average images with unseeded helium fuel simulant: a) straight and b) low-swirl cases.

ice particles which, on the basis of observed light scattering levels and marker shot noise, were calculated to be of the order of 50 nm in diameter.[13] Light scattering from these particles was typically an order of magnitude greater in intensity than scattering from the air. The particles were sufficiently small that they followed the flow, their mass fraction was small enough ($\sim 5 \times 10^{-4}$ fraction in helium) that they did not effect the density, and the heat release due to their condensation in the injector nozzles produced a negligible ($\sim$0.2 K) temperature rise. Consequently, these particles are an effective and nonintrusive marker of the fuel simulant.

Images of the flow at four sections, as shown in Fig. 3, were acquired. The first section was a plane parallel to the side walls of the duct through the centerline of the fuel injector; the other sections were planes normal to the duct axis at x/d = 7.8, 15.8, and 23.8. The duct, which discharged directly to the atmosphere, had interchangeable wall pieces that allowed its length to be changed so that flow visualization, which took place in the immediate vicinity of the duct exit, could be performed at these various locations. (Note that in these various buildups the location of the fuel injector relative to the facility nozzle exit is unchanged.) The section at the

injector was achieved by assembling the duct to just upstream of the fuel injector on three sides, and longer on the fourth side where the fuel injector was located. The field of view (FOV) was from $x = -0.15$ to 0.90 in. and from $z = 0$ to 1.05 in. Since the main flow pressure was matched to atmospheric, waves that formed at the exit of the duct at the three shorter sides were weak. The wave that extended from the end of the opposite wall passed above and to the right of the top right-hand corner of the FOV, and waves from the end of the side walls did not intersect the fuel plume until still farther downstream. Consequently, we believe the flow within the FOV is essentially as it would be if the duct were built up to its full length. The remaining sections were achieved by assembling all four sides of the duct to an equal length (which differed for each x/d) and locating the light sheet 0.2 in. downstream of the duct exit. The camera looked down on the exit of the duct through a 90-deg turning mirror placed at the edge of the jet flow. The FOV was from $y = -0.75$ to 0.75 in. and from $z = -0.1$ to 1.45 in. Wall pressures measurements obtained with the duct built up to various heights were compared to each other,[13] and, in more recent work,[15] schlieren images of the flow within the duct at its maximum height have been compared with laser sheet images obtained at the exit for various buildup heights. All results indicate no effect of buildup height on the internal flow.

Images were captured and digitized by a cooled charge-coupled device camera connected to a personal computer with 512 × 512 pixels binned 2 × 2 (to improve signal-to-noise ratio) and 35% quantum efficiency at 266 nm. The images were composed of 16-bit data (65,536 gray levels) with a digitization noise of about 20 electrons rms during facility operation. The FOV was imaged by a commercial $f4.5$, 105-mm focal-length camera lens with extension tubes. Sequences of single laser pulse images and 60 laser shot averages were acquired for all cases, with and without water-seeding. The effects of background light and light-sheet nonuniformities were corrected by subtraction of a background image and division by a reference image. The small amount of distortion inherent in the images due to the viewing angle was corrected by image processing and bright spots in images caused by large dust particles were removed. The images that result have pixel intensity values that are proportional to scattering cross section, with errors arising from imperfect correction for background light and light-sheet nonuniformities, and also from camera digitization and photon shot noise. Errors in the background were probably less than 10% of image full scale and errors in referencing on the order of 10–15% of the local value. For single laser shots, the ratio of signal to rms camera noise was in the range of 8–12 in the airstream region of the flow, for 60 shot averages it was 5–10 times larger.

Results

Unseeded Jets

Figures 3a and 3b are three-dimensional views, to scale, showing the 60-shot-average images obtained with helium injection, the outline of the exit of the fuel simulant nozzle, and the interior edges of the duct. Figure 3a is for the straight (straight insert) case and Fig. 3b is for the low-swirl (low-swirl insert) case. A number of features are visible in both figures: the helium jet and the plume formed as the jet turns parallel to the main flow, the bow shock and its reflection from the opposite wall, and the boundary layer on the injection wall. The boundary layer on the far wall is not seen due to the limited FOV.

It is well known that a jet without swirl injected at 30 deg into a crossflow forms a plume with an embedded counter-rotating vortex pair with common flow away from the wall. In the straight case the plume was symmetrical about the x–z plane: at $x/d = 7.8$ two lobes formed by the vortex pair can be seen within the core; at $x/d = 15.8$ and 23.8 the plume was essentially circular in cross section. By contrast, in the low-swirl case the plume behaved like a single streamwise vortex with clockwise rotation (consistent with the sense of rotation of the swirling jet) interacting with its images in the walls. As a result, the axis of the major portion of the plume was inclined to the x–z plane at an angle estimated to be about 2.5 deg from the images shown in Fig. 3b. The flow of the air around the jet in the vicinity of injection is probably somewhat similar to that around a cylinder mounted to a surface in a crossflow. If the cylinder is made to spin, the boundary layer on the cylinder separates asymmetrically, giving rise to circulation around the body and generating lift (the Magnus effect[16]); without spin, of course, there is no circulation. The circulation of the jet is conserved as it turns over to form the plume so that the plume behaves like a longitudinal vortex. Note that asymmetrical longitudinal vortices in a fuel-simulant plume have been observed previously, e.g., Fuller et al.[11] for downstream-angled injection with yaw into a supersonic freestream.

The plume circulation for the low-swirl case with helium fuel was estimated by assuming that the lateral motion of the center of the plume, between $x/d = 7.8$–23.8, could be modeled by the motion of a point vortex in a two-dimensional, irrotational flow interacting with its images in the surfaces. This assumption is plausible in a fuel plume with little shear (not really true for the helium cases) and provided crossflow Mach numbers are small (slender flow, a reasonable assumption where it was applied). The lateral velocity was taken to be $u_\infty \tan(2.5 \text{ deg})$, and images in the injection and opposite walls, and images of the walls, ad infinitum, were considered. The circulation was found to be about $0.33\pi u_\infty d$, 43% of the circulation contained within the swirling flow in the fuel simulant nozzle ($\pi d v_\theta$). Because the axial velocity within the plume and the airstream probably differ substantially, it is possible that this estimate of the circulation of the fuel plume is inaccurate. However, injection of a swirling jet does appear to be an effective method for generating a streamwise vortex. The other swirling cases (high swirl with helium and low swirl with air) seemed to behave in a similar fashion, but no estimates of circulation were made in these cases because of difficulties in defining the plume center with the available data.

Seeded Jets

This section presents results of the experiment in which the fuel simulant was seeded to obtain information on the penetration and growth of the fuel plume. As discussed earlier, the quantity of water added is tiny (and so does not change the flow), and the particles formed follow the flow. Figure 4 shows typical single-laser-pulse images in the section at the fuel injector with helium fuel simulant; the main flow is from left to right. The top images are for the straight case while the bottom are for the low-swirl case, and the left-hand-side (LHS) images are for unseeded helium while the right-hand side (RHS) are for seeded helium. In the images with unseeded helium the bow shock (upstream of the jet) is clearly seen extending from bottom left to top right. Acoustical waves emanating from mixing layer eddies are visible in the airstream. Because of the low scattering cross section of helium the fuel jet is dark, and the difference between the two cases with unseeded helium is no more than the shot-to-shot variation for a given case. In the water-seeded, straight case the condensation fills the jet, revealing a low-turbulence core and a recompression shock extending downstream and away from the wall at the downstream edge of the jet. In the low-swirl and high-swirl (not shown) cases, near the injection point, scattering is visible in the outer part of the jet, but not in the core. The absence of scattering particulates in the core is probably due to the lower pressure and higher temperature, which leads to reduced or eliminated condensation. The condensation-core interface is quite smooth near the nozzle exit,

suggesting that turbulence levels in the core were low, or at least the length scales were small. This result is consistent with an expected stabilizing gradient of angular momentum within the core of the swirling jet.[17] Downstream of the point where the jet turns parallel to the duct main flow, the interface is more ragged, presumably as a result of instability of the swirling jet in the presence of strong, asymmetrical pressure gradients. The core closes off by the RHS of the image due to growth of the condensation-filled region. Note that vortex instability and the generation of turbulence are both characteristics of vortex breakdown; however, flow reversal along the vortex axis, another characteristic of breakdown, was not obviously apparent in the images acquired.

The convective Mach number[1] of the straight jet mixing layer near the point of injection was estimated based on u_j, and the velocity on a 30-deg cone in an airflow with the same Mach number, temperature, and pressure as the duct flow. For helium fuel simulant it was about 1.2, but for air it was only about 0.3. The orientation of the acoustical waves seen in Fig. 4 (inclined backwards at roughly 45 deg) indicates that the eddies are moving right-to-left at supersonic speeds with respect to the airstream, consistent with the high convective Mach number predicted for helium injection. Acoustical waves were not visible for air injection, as expected. Previous observations have indicated that compressible mixing layers are more three dimensional and less periodic in the structure,[18] and indeed, the eddies in the mixing layer ahead of the point where the jet turned over seemed less regular or periodic for helium injection than for air. Mixing-layer visual growth rates in this region could not be accurately assessed from the images, but there appeared to be no large effect of either fuel simulant type or swirl. The correlations of Papamoschou and Roshko,[1] based on data for nonswirling flow, indicate growth rates for the straight cases that are almost the same for helium fuel simulant as for air, in the range 0.05–0.06, the tendency for the greater shear with the helium jet to produce a greater mixing-layer growth rate is apparently offset by the tendency of greater compressibility effects to reduce it. However, the lack of effect of swirl (if true) appears inconsistent with previous results on the effect of swirl on mixing in supersonic jets, which suggested a significant increase in mixing-layer growth rate with swirl.[4–6]

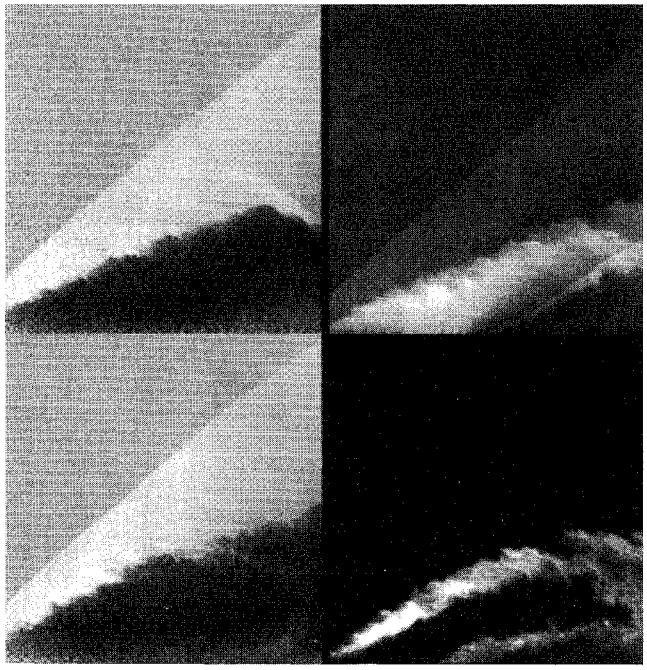

Fig. 4 Typical images at the injector with helium fuel simulant: straight case (top left), straight case with seeding (top right), low-swirl case (bottom left), and low-swirl case with seeding (bottom right).

Figures 5a and 5b show typical single-shot images looking upstream for the straight and low-swirl cases with helium fuel simulant, at, respectively, x/d = 7.8 and 23.8. Comparison between the images in which helium has been seeded with water (on the right) with images in which it has not (on the left) suggest that water condensation occurred everywhere there was any significant amount of helium (except with swirl, in the core near the point of injection, as discussed earlier). In all cases the helium plume was very ragged and unsteady. Additional features can be seen in the images with unseeded fuel, including (faintly) shocks and the boundary layer on the fuel injector wall. (Note that the bottom edge of the image is the wall.) Images such as these were analyzed to estimate penetration and mixing efficiency.

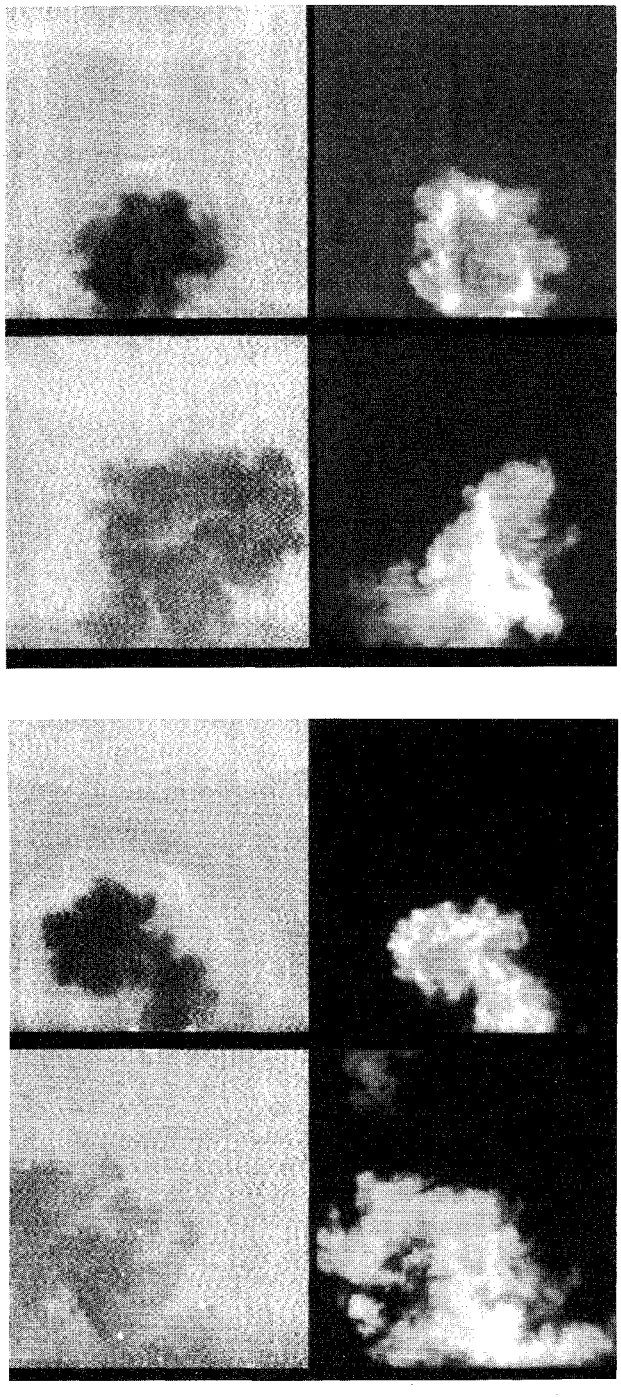

Fig. 5 Typical images with helium fuel simulant: at top x/d = 7.8 and at bottom 23.8; on the right the helium is seeded: a) straight and b) low-swirl cases.

Table 2 Parameters derived from the images

	Straight			Low swirl		High swirl
	Air	Air, 2×	Helium	Air	Helium	Helium
A_p/A_j, x/d = 7.8	4.7	4.8	7.1	4.3	7.2	6.9
x/d = 15.8	6.2	8.4	10.3	7.1	11.4	10.7
x/d = 23.8	7.5	12.9	11.4	11.5	14.3	15.9
z_p/d, x/d = 7.8	1.43	2.04	1.55	1.41	1.54	1.46
x/d = 15.8	1.97	2.45	1.73	1.56	1.94	1.57
x/d = 23.8	2.35	3.21	2.18	1.63	1.94	2.03

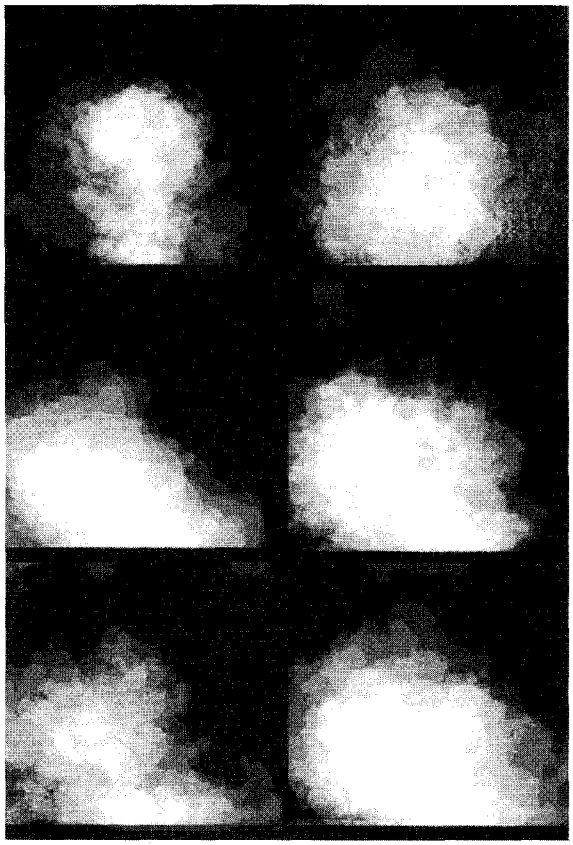

Fig. 6 Average of thresholded images at x/d = 23.8. Straight cases (top), low-swirl cases (middle), and high-swirl cases (bottom) are shown, with air fuel simulant on the LHS and helium on the RHS.

Quantitative Analysis of Images

Histograms of single laser pulse images with seeded fuel simulant had two peaks corresponding to the most likely to occur intensity in the airstream and the most likely to occur intensity in the fuel simulant plume. Each image was thresholded, with the cutoff intensity value being the airstream peak of the histogram plus 100/255 of the distance between the peaks. Pixels with intensity values above the cutoff had intensity set to 1 while the remaining pixels had intensity set to 0. Since the boundary of the plume was distinct, thresholded images were relatively insensitive to the cutoff value. A sequence of 6–10 images obtained at different times was averaged to obtain an image of intermittency, the fraction of time that fuel simulant occurred in any nonzero fraction. Several images of intermittency at x/d = 23.8 are shown in Fig. 6. Straight cases (with matched pressure), low-swirl cases, and high-swirl cases are shown, respectively, from top to bottom. The images on the LHS are for air fuel simulant and those on the right are for helium. In general, the air fuel simulant spreads to occupy a smaller cross-sectional area, while the penetration distance from the wall for air and helium is generally similar. With the addition of swirl the fuel plumes appear to lean to the left, as noted earlier, with little obvious difference in degree of lean between low and high swirl and between air and helium fuel simulant.

By counting the number of pixels above the threshold for each individual thresholded image, multiplying by the duct area per pixel, and averaging over the sequence, the average cross-sectional area occupied by the plume A_p was found. This procedure was repeated at each streamwise location, and the results normalized by jet nozzle exit area. Note that at the last location (x/d = 23.8) for the swirling cases, the fuel plume intermittently extended beyond the left-hand edge of the FOV, so that A_p was slightly underestimated for these cases. The penetration z_p, defined as the z location of the c.m. of the intermittency, was obtained from the intermittency image at each section. These results are given as a function of x/d for all of the various cases in Table 2.

For the helium cases, swirl produced an increase in A_p/A_j at the last streamwise location, but it produced little change at upstream locations. For air cases, swirl produced a slightly greater relative increase in A_p/A_j at both x/d = 15.8 and 23.8. A_p/A_j was consistently greater for helium than for air, notwithstanding the initially similar mixing-layer growth rates observed earlier, presumably because the effects of shear persist farther downstream when it is initially higher. (Note that, as shown in Table 1, u_j/u_∞ is similar among cases with a given fuel simulant, but is more than twice for helium as for air.) The effect of doubling the fuel pressure, and consequently, doubling the mass flow rate of fuel simulant, is a substantial increase in A_p/A_j.

For the pressure-matched jets, penetration in the region $x/d < 5$–10 appears to scale primarily upon fuel jet exit diameter, i.e., is constant in this experiment. Downstream of this the rate of increase in penetration is probably dependent both upon (inviscid) vortex interactions and upon the spreading that occurs as a result of turbulent mixing. For the straight jet case a counter-rotating vortex pair was generated, and the vortices interacted with each other, causing themselves and the fuel plume to move away from the wall, thus increasing penetration. With swirl, the plume contained only one dominant vortex, causing lateral motion as described previously, but not acting to enhance penetration. Thus, with air fuel simulant, where shear was low and vortex interaction was the major mechanism for causing the fuel to move away from the wall in the downstream region, the rate of increase of penetration with downstream distance was greater without swirl. With helium fuel simulant, where shear was greater and turbulent mixing was an important mechanism (and may in fact have acted to weaken the vortex interaction by causing the vortices to move apart and/or causing cross diffusion and cancellation of vorticity between the two vortices), there was little effect on penetration of swirl. When the jet pressure was doubled, in the case of air fuel simulant, penetration in the region $x/d < 5$–10 was substantially increased as was the downstream slope.

Results in which x, z_p, and A_p are renormalized by $A_{\text{eff}} \equiv \dot{m}_j/(\rho_\infty u)$ and $d_{\text{eff}} \equiv 2\sqrt{(A_{\text{eff}}/\pi)}$, following Ref. 11, are shown in Figs. 7 and 8. The purpose of this renormalization is not necessarily to collapse the data, but rather to allow comparison of cases on the basis of equal mass flow, rather than

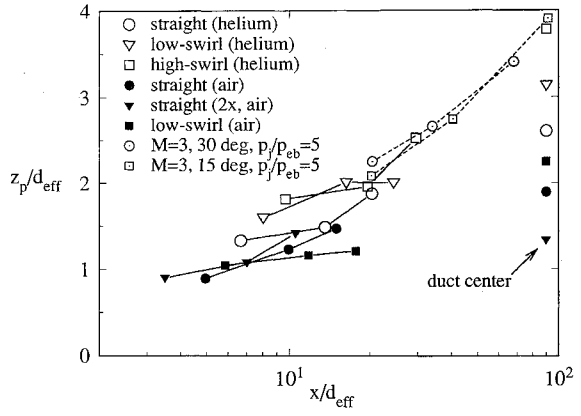

Fig. 7 Plume penetration: the present cases and cases due to Fuller et al.[11]

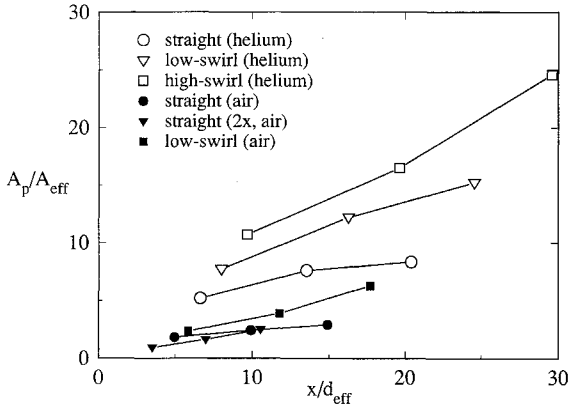

Fig. 8 Plume average cross-sectional area.

equal injector diameter. Ultimately, of course, in a scramjet combustor, a specified mass of fuel will have to be injected and mixed, since penetration (whether scaled by d or, as is shown later, d_{eff}) is roughly similar for straight and swirl injectors. The injector that mixes a specified mass of fuel to stoichiometry in the shortest streamwise distance is favored. Figure 7 shows that after renormalization the effect of swirl was to slightly increase penetration for helium fuel and to slightly decrease it for air fuel. Also shown in Fig. 7 are data points obtained from Ref. 11 for sonic injection of helium into a Mach 3 airstream: 30-deg injection with $p_j/p_{eb} = 5$; and 15-deg injection with $p_j/p_{eb} = 5$. In Ref. 11, the penetration was defined as the distance from the injector wall of the location of peak fuel simulant concentration, a definition effectively similar to our own. The results are at larger x/d_{eff} than the present ones, but are generally consistent, although a third case from Ref. 11 (15-deg injection with $p_j/p_{eb} = 1$) had much lower penetration. As shown in Fig. 8, A_p/A_{eff} was much larger for helium fuel simulant than for air, and was substantially increased by addition of swirl. In the straight case, with air fuel simulant, there was little effect on A_p/A_{eff} of doubling fuel simulant pressure.

Note that, in rescaling on the basis of d_{eff} and A_{eff} and comparing between cases, it has implicitly been assumed that there is no effect of confinement on penetration and plume cross-sectional area. In fact, penetration is ultimately limited by the opposite wall to somewhere between the full duct height and the duct center, and plume area is limited by duct cross-sectional area. (As a reference point, the duct center, which in the rescaled coordinates varies from case to case, is indicated in Fig. 7 by the points at $x/d_{eff} = 90$.) It is unlikely there was any effect of confinement on results at the first data plane (at $x/d = 7.8$), which was ahead of the point at which the reflection of the bow shock from the opposite and side walls intersected the fuel plume. The effect of the reflected bow shock is to turn the plume towards the wall, so that the penetration at data planes downstream of $x/d = 7.8$ is probably less than in an unconfined flow. Unfortunately, there is no simple way, based on the available data, to estimate the magnitude of this effect on penetration, which presumably varied from case to case. It is clear that if the slopes of the curves in Fig. 7 were increased the collapse of the penetration data would be improved: however, this is not in itself evidence that the slopes would be steeper. The effects of confinement on the plume cross-sectional area are expected to be less, provided the plume does not directly contact the opposite wall boundary layer, since the rate of growth is probably governed by turbulent processes, rather than the inviscid effects of the pressure field.

It is evident from Fig. 8 that addition of swirl and reduction of fuel simulant density (hence, increase of shear) both produced a considerable increase of plume cross-sectional area at a given streamwise station, probably as a result of greater mixing. An increase in mixing associated with increase in shear is obvious. There are several possible explanations for an increase in mixing with swirl, and more than one of these may have been significant. Previous studies of mixing-layer growth in compressible mixing layers surrounding swirling, axisymmetric, supersonic jets have shown that swirl can delay to higher Mach numbers, or inhibit, the deleterious effects of compressibility on mixing-layer growth rate.[4,6] In Ref. 4 a more than three times increase in mixing-layer growth rate over that of the nonswirling jet was observed in one of the cases, and results were correlated in terms of gradient Richardson number.[17] It was pointed out that for an axisymmetric swirling jet into a nonswirling coflow, the destabilizing effect of radial angular momentum gradient is greater than any possible stabilizing effect of radial density gradient, so that this case is unstable. Therefore, the swirl effects on mixing-layer growth rate could be responsible for an increased mixing. The overall stirring motion coupled with the nonaxisymmetry of the flow in the mean, leading to greater fuel-air interfacial area, may also have contributed to an increased mixing, as may the greater levels of turbulence in the vicinity of the injection point. Some of these mechanisms should be relatively less important farther downstream: the effects of additional turbulence generated at the point of injection will dissipate and the increase in mixing-layer growth rate produced by swirl will decrease as the convective Mach number becomes low. However, there is no particular evidence for this in the data.

Conclusions

The effects of swirl upon the mixing of 30-deg helium and air wall jets injected into a confined Mach 2 airflow, simulating fuel injection into a scramjet combustor, were investigated. The flowfield in the duct was visualized by imaging scattering from a laser light sheet, in some cases, scattering in the fuel-simulant plume was enhanced by seeding it with water vapor that condensed to provide scattering particulates. It was shown that the addition of swirl resulted in a dominant streamwise vortex within the fuel-simulant plume, causing the plume to move laterally. Fuel-simulant penetration and average cross-sectional area of the plume were calculated by thresholding the seeded fuel images, and it was shown that addition of swirl increased fuel plume cross-sectional area (for given mass flow), most probably due to increased mixing, while the effects on penetration were smaller. Finally, it should be mentioned that any improvement in mixing due to swirl comes at some cost, since higher fuel supply pressures are required to produce swirling jets of a given nozzle exit pressure and axial velocity. It is left to future studies to show whether the gains in mixing more than offset the losses incurred in achieving the greater mixing.

Acknowledgments

Both authors received financial support under NASA Cooperative Agreement NCC1-24, and the second author received support under NASA Contract NAS1-19699. The assistance of G. B. Northam and the staff of the NASA Langley Research Center, whose equipment and facilities were used, is gratefully acknowledged.

References

[1]Papamoschou, D., and Roshko, A., "The Compressible Turbulent Shear Layer: An Experimental Study," *Journal of Fluid Mechanics*, Vol. 197, 1988, pp. 453–477.

[2]Cutler, A. D., and Levey, B. S., "Vortex Breakdown in a Supersonic Jet," AIAA Paper 91-1815, June 1991.

[3]Levey, B. S., "An Experimental Investigation of a Supersonic Vortical Flow," M.S. Thesis, School of Engineering and Applied Science, George Washington Univ., Washington, DC, Sept. 1991.

[4]Cutler, A. D., Levey, B. S., and Kraus, D. K., "Near-Field Flow of Supersonic Swirling Jets," *AIAA Journal*, Vol. 33, No. 10, 1995; also Cutler, A. D., Levey, B. S., and Kraus, D. K., "An Experimental Investigation of Supersonic Swirling Jets," AIAA Paper 93-2922, July 1993.

[5]Naughton, J. W., and Settles, G. S., "Experiments on the Enhancement of Compressible Mixing via Streamwise Vorticity, Part I—Optical Measurements," AIAA Paper 92-3549, July 1992.

[6]Naughton, J. W., and Settles, G. S., "A Theoretical Framework for Mixing Layers Surrounding Compressible Swirling Jets," AIAA Paper 94-2245, June 1994.

[7]Delery, J., Horowitz, E., Leuchter, O., and Solignac, J. L., "Fundamental Studies on Vortex Flows," *La Recherche Aerospatiale*, No. 1984-2, 1984, pp. 1–24.

[8]Cattafesta, L. N., III, and Settles, G. S., "Experiments on Shock/Vortex Interaction," AIAA Paper 92-0315, Jan. 1992.

[9]McClinton, C. R., "The Effect of Injection Angle on the Interaction Between Sonic Secondary Jets and a Supersonic Free Stream," NASA TND-6669, Feb. 1972.

[10]Mays, R. B., Thomas, R. H., and Schetz, J. A., "Low Angle Injection into a Supersonic Flow," AIAA Paper 89-2461, July 1989.

[11]Fuller, E. J., Mays, R. B., Thomas, R. H., and Schetz, J. A., "Mixing Studies of Helium in Air at High Supersonic Speeds," *AIAA Journal*, Vol. 30, No. 9, 1992, pp. 2234–2243.

[12]Riggins, D. W., and McClinton, C. R., "Analysis of Losses in Supersonic Mixing and Reacting Flows," AIAA Paper 91-2266, June 1991.

[13]Kraus, D. K., "An Experimental Investigation of Mixing Enhancement in a Simulated Scramjet Combustor by Use of Swirling Jets," M.S. Thesis, School of Engineering and Applied Science, George Washington Univ., Washington, DC, Aug. 1993; also Kraus, D. K., and Cutler, A. D., "Mixing Enhancement by Use of Swirling Jets," AIAA Paper 93-3126, July 1993.

[14]Papamoschou, D., and Hubbard, D. G., "Visual Observations of Supersonic Transverse Jets," *Experiments in Fluids*, Vol. 14, 1993, pp. 468–476.

[15]Johnson, C. H., M.S. Thesis, School of Engineering and Applied Science, George Washington Univ., Washington, DC, Aug. 1995.

[16]Gilmore, C. P., "Spin Sail," *Popular Science*, Vol. 224, No. 1, 1984, pp. 70–73.

[17]Bradshaw, P., "Effects of Streamline Curvature on Turbulent Flow," AGARDograph 169, Aug. 1973.

[18]Clemens, N. T., and Mungal, M. G., "Two- and Three-Dimensional Effects in the Supersonic Mixing Layer," *AIAA Journal*, Vol. 30, No. 4, 1992, pp. 973–981.